

# Extra electron reflections in concentrated alloys may originate from planar defects, not short-range order

Flynn Walsh,<sup>1,2</sup> Mingwei Zhang,<sup>1,3,4</sup> Robert O. Ritchie,<sup>1,4</sup> Andrew M. Minor,<sup>1,3,4</sup> and Mark Asta<sup>1,4,\*</sup>

<sup>1</sup>Materials Sciences Division, Lawrence Berkeley National Laboratory, Berkeley, CA 94720

<sup>2</sup>Graduate Group in Applied Science & Technology, University of California, Berkeley, CA 94720

<sup>3</sup>National Center for Electron Microscopy, Lawrence Berkeley National Laboratory, Berkeley, CA 94720

<sup>4</sup>Department of Materials Science & Engineering, University of California, Berkeley, CA 94720

In many concentrated alloys of current interest, the observation of diffuse superlattice intensities by transmission electron microscopy has been attributed to the presence of chemical short-range order. This interpretation is questioned on the basis of crystallographic considerations and theoretical predictions of ordering. The work of Xiao and Daykin [*Ultramicroscopy* **53** (1994)], which shows how planar defects can produce the exact set of observed peaks, is highlighted as an alternative explanation that would impact the conclusions of a number of recent studies.

The chemical short-range order (SRO) of face-centered cubic (fcc) alloys containing significant concentrations of several  $3d$  elements—especially “medium-entropy” VCoNi and CrCoNi—has been extensively studied in recent years, e.g. Refs. [1–14]. While there is little evidence that SRO can be controlled to tailor the bulk mechanical properties of these materials [5, 7, 14], it has been argued that an essentially ubiquitous degree of Å-scale order could nonetheless play an important role in a wide range of properties [1, 8, 12]. For example, many alloys containing Co are predicted to form hexagonal close-packed lattices at ambient conditions [15, 16], but quenched-in SRO could explain the persistent metastability of the fcc phase [1, 8, 12].

This view appears to be corroborated by recent transmission electron microscopy (TEM) purporting the presence of local order in a variety of samples subject to minimal thermal processing beyond high-temperature homogenization. Perhaps most notably, Chen et al. [10] proposed the existence of SRO in VCoNi on the basis of diffuse intensities at  $\frac{1}{2}\{311\}$  superlattice points in reciprocal space while imaging in the  $[\bar{1}12]$  zone axis (ZA), i.e. the direction of electron beam incidence. An equivalent electron diffraction pattern is shown in Fig. 1. Some of the same authors [10] later reported additional intensities at  $\frac{1}{3}\{422\}$  in the  $[\bar{1}11]$  ZA [10]. Similar observations have at various points been attributed to SRO in a Cr-Ni-based alloy [17], CrCoNi [11, 14], and Mn-rich steels [18–20]. Diffuse superlattice peaks have also been found in the  $[\bar{1}11]$  ZA of the CrMnFeCoNi high-entropy alloy [21, 22], although these were considered to possibly represent static lattice displacements rather than SRO.

Considered individually, the reported reflections are not inconsistent with the partial formation of a CuPt-type ( $L1_1$ ) concentration wave involving the compositional enrichment and depletion of alternating  $\{111\}$  (and simultaneously  $\{311\}$ ) planes, as illustrated on the left-hand side of Fig. 2. In VCoNi and CrCoNi, the microscopy was interpreted to reflect modulations of V

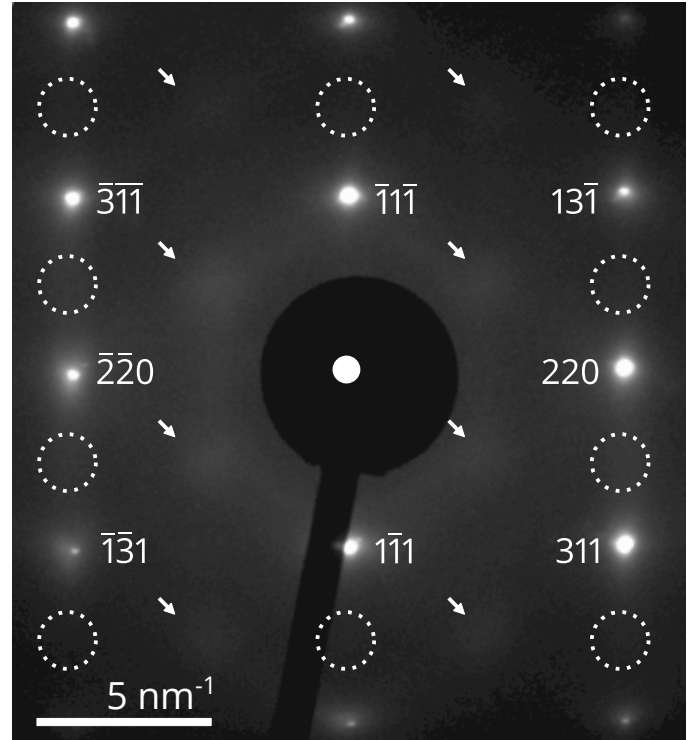


FIG. 1: Experimental [14] electron diffraction pattern of CrCoNi in the  $[\bar{1}12]$  ZA, as is representative of literature results for alloys discussed in the text. Diffuse intensities at  $\frac{1}{2}\{311\}$  superlattice positions are marked with arrows, but there are no peaks at  $\frac{1}{2}\{111\}$  sites, as highlighted by the dotted circles.

or Cr concentrations in this manner [9–11], largely on the basis of electronic structure calculations indicating repulsive interactions between V-V and Cr-Cr neighbors, although we note that CuPt-type ordering has the same nearest neighbor pair frequencies as a random alloy. Some efforts have been made to support this theory with atomic scale composition mapping [9, 11], but, in contrast to the diffuse intensities themselves, these measurements hardly seem statistically conclusive.

\* mdasta@berkeley.edu

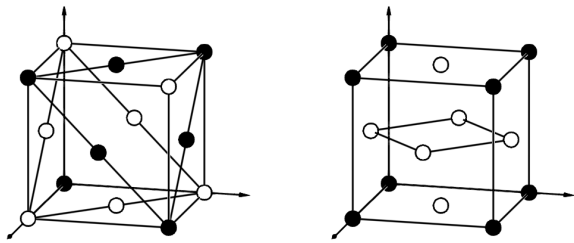


FIG. 2: *Left:* The CuPt ( $L1_1$ ) unit cell. SRO of this form has been proposed for VCoNi and CrCoNi with V or Cr-rich  $\bullet$  sites and complementarily depleted  $\circ$  sites on alternating (111) planes. *Right:* Similarly, an  $AlNi_3$  ( $L1_2$ ) unit cell. First-principles calculations suggest that this type of ordering, in which V or Cr-rich  $\bullet$  sites form a sublattice that minimizes nearest neighbors, should be far more energetically favorable, if not the ground state, in these systems [2, 3].

However, interpretations of order are questionable on several accounts, most notably the absence of additional expected peaks. By the symmetry of the fcc lattice, a CuPt-type decoration can equivalently occur in four rotational variants, corresponding to order on either  $(\bar{1}11)$ , (111),  $(11\bar{1})$ , or  $(1\bar{1}\bar{1})$  planes, with four additional antiphase structures that are redundant for purposes of diffraction. The four rotational variants are illustrated in the top row of Fig. 3 from the perspective of the  $[\bar{1}12]$  ZA, with atomic columns shaded by composition; the reciprocal space peaks expected from each variant are shown below for the same ZA. (Reflections were determined from the basic diffraction criterion for concentration waves [23], as restricted by the two-dimensional nature of TEM, and explicitly verified through Prismatic [24] simulations.)

As illustrated in Fig. 3(a), the  $\frac{1}{2}\{311\}$  peaks visible in Fig. 1 are associated only with the  $(\bar{1}11)$  variant. While the variants on (111) and  $(11\bar{1})$  planes are not expected to produce additional reflections in this orientation, the  $(1\bar{1}\bar{1})$ -based variant depicted in Fig. 3(d) should be readily visible, as it would involve composition modulation across the  $(1\bar{1}\bar{1})$  planes that form the rows of atomic columns viewed in TEM. Nonetheless, the associated  $\frac{1}{2}(1\bar{1}\bar{1})$  peaks are missing from all experimental characterizations of the  $[\bar{1}12]$  ZA, through either electron diffraction or the Fourier transformation of dark-field images [9–11, 14, 17–20]. Locations where additional reflections would be expected are circled in Fig. 1 and marked in Fig. 3(d). Given the quantity of material sampled across numerous studies, the absence of a variant is not statistically conceivable. One could attempt to construct an alternative structure giving rise to only  $\frac{1}{2}\{311\}$  intensities, but every  $\frac{1}{2}\{311\}$  peak is related to a  $\frac{1}{2}\{111\}$  spot by a  $\{200\}$  reciprocal lattice vector, e.g.  $\frac{1}{2}(131) - (020) = \frac{1}{2}(1\bar{1}\bar{1})$ , as is the case of Fig. 3(d).

TABLE I: Extra electron reflections expected from planar defects within an fcc lattice per Xiao and Daykin [25]<sup>a</sup>. Their predictions match the observations of many experimental studies, as noted for each ZA. In most cases, the intensities were originally attributed to SRO.

ZA	Predicted intensities	Observations
[011]	streaking	[4, 17]
$[\bar{1}11]$	$\frac{1}{3}\{422\}$	[10, 17, 20–22]
$[\bar{1}12]$	$\frac{1}{2}\{311\}$	[9–11, 14, 17–20]
[013]	$\frac{1}{2}\{13\bar{1}\}, \frac{1}{2}\{33\bar{1}\}$	[20]
$[\bar{1}14]$	$\frac{1}{2}\{3\bar{1}1\}, \frac{1}{2}\{511\}, \frac{1}{3}\{442\}$	—

<sup>a</sup> The originally tabulated  $\{200\}$  spots in the [001] ZA are fcc lattice reflections and hence omitted here.

Since the diffraction criterion for concentration waves is independent of reciprocal lattice translations [23], any ordering that produces  $\frac{1}{2}\{311\}$  peaks should also effect  $\frac{1}{2}\{111\}$  intensities as long as all variants are present.

Intriguingly, the same phenomenon, in which  $\frac{1}{2}\{311\}$  peaks appear without  $\frac{1}{2}\{111\}$  intensities, has been previously observed by Xiao and Daykin [25], who studied stacking faults in pure Si. These authors detailed how the presence of planar defects, namely stacking faults and nanotwins, leads to the same forbidden reflections in diamond cubic and fcc lattices, which are summarized in Table I. Remarkably, Xiao and Daykin [25] predicted the exact set of extra peaks that have been reported in the  $[\bar{1}12]$ ,  $[\bar{1}11]$ , and [013] ZAs of concentrated alloys, offering an alternative explanation for the experimental findings described above. Published observations in the [011] ZA also seem to support this picture—CuPt-type ordering should produce additional superlattice reflections in this ZA, which are generally not observed [4, 9, 11]. (Chen et al. [10] claim to detect faint intensities at  $\frac{1}{2}\{111\}$ , but these do not seem distinguishable from the surrounding noise.) We have only ever observed streaking in this ZA, as seen in Ref. [4], which would also be consistent with planar defects [25].

Of course, the obvious objection to this hypothesis is that the experimental samples appeared to contain no structural imperfections in the examined regions. Considering that these features are usually quite visible under TEM, some explanation of how presumably nanoscale planar defects could otherwise escape detection is required to prove their generation of the observed peaks. Still, experimental intensities are far more consistent with changes in the stacking sequence than SRO.

Further challenging assumptions of SRO, the experimental intensities are largely inconsistent with the predictions of density-functional theory, either directly or through parameterized interatomic potentials. As previously noted [11, 13], CuPt-type ordering is energetically unfavorable in otherwise similar V-Ni or Cr-Ni alloys. In these systems, experimental SRO has been primarily interpreted in terms of  $AlNi_3$  ( $L1_2$ , see Fig. 2) or

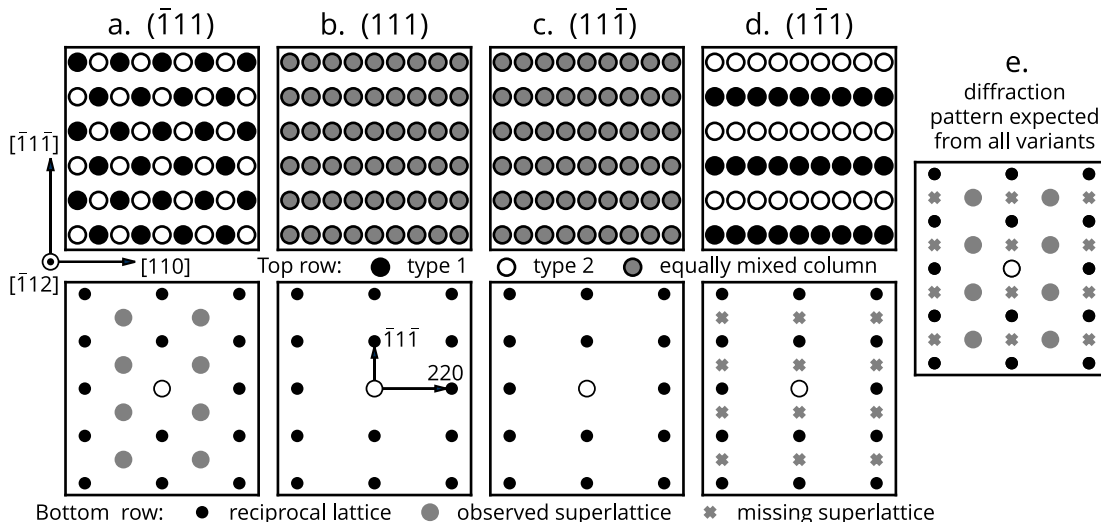


FIG. 3: (a-d) The four rotational variants of a CuPt-type structure, consisting of ordering on the denoted planes.

In the top row, the structures are drawn from the perspective of the  $[\bar{1}12]$  ZA, with columns of atoms shaded according to the average composition. (In CuPt, types 1 and 2 would simply represent columns of Cu and Pt; in recently proposed SRO, they correspond to Cr or V enrichment and depletion as in Fig. 2.) The reciprocal space signatures of the four variants, as would be obtained by Fourier transforming a dark-field image or electron diffraction, are shown below for the same ZA. (e) The expected experimental electron diffraction pattern, which should contain superlattice intensities corresponding to all variants. Only those associated with variant (a) have been reported in the discussed alloys, questioning the existence of this form of order.

$\text{Al}_3\text{Ti}$ -type ( $\text{DO}_{22}$ ) concentration waves [26–29], both of which minimize nearest neighbors among the ordering solute. CuPt-type intermetallics, on the other hand, rarely form outside of noble metal systems. First-principles calculations consistently indicate that VCoNi and CrCoNi should order similarly to the aforementioned binaries, with VCoNi clearly favoring an  $\text{AlNi}_3$ -type V sublattice [3] and similar (though not identical) preferences noted for CrCoNi [6, 8, 13]. (Verifying this point, we have calculated how CuPt-type concentration waves explicitly raise the energy of random VCoNi and CrCoNi solutions regardless of the degree of order, which will be detailed in a forthcoming study.)

Even if the experimental form of high-temperature SRO unexpectedly differed from theoretical predictions, a structure reducing Cr-Cr or V-V neighbors would still be expected from electrostatic considerations arising from charge transfer among elements with half-empty (Cr, V) and mostly full (Ni, Co)  $3d$  orbitals [30]. In practice, the basic predictions of electronic structure calculations are largely supported by diffuse X-ray scattering in CrFeCoNi, which reveals an incipient  $\text{AlNi}_3$ -type Cr sublattice [2] after long-term aging at low temperatures. Moreover, VCoNi alloys readily form fully ordered  $\text{AlNi}_3$ -type domains (see Fig. 2), which were observed alongside the nominally disordered regions used for the characterization of SRO by Ref. [9]—it would be unexpected for this material to host SRO corresponding to a completely different structure immediately adjacent to the theoret-

cally predicted phase.

Du et al. [13] exhaustively studied the thermodynamics and kinetics of ordering in CrCoNi through Monte Carlo simulations of ensembles described by a carefully parameterized interatomic potential. While noting the energetic unfavorability of a CuPt-type structure, they attempted to explain experimental results [11] by identifying local instances of the structural motif in high-temperature simulations. However, corresponding diffraction patterns were not provided and it is unclear if these regions represent anything beyond random fluctuations. Their frequency does not vary with temperature above the point of long-range ordering and equivalent instances of theoretically favorable  $\{100\}$  and  $\{110\}$ -based motifs are consistently more prevalent, even though their associated peaks are not found experimentally.

Altogether, there seems to be little theoretical basis for any form of SRO consistent with the electron diffraction of VCoNi, CrCoNi, and other similar alloys, while the reported features consistently match those expected from changes in the stacking sequence [25]. On the weight of the circumstantial evidence, we believe that assumptions of ordering should be revisited and the possibility that planar defects produced the observed diffuse intensities deserves serious consideration. This is not to say that experimental samples necessarily lacked SRO, simply that it may not be detected by the employed techniques; the extent of ordering required to produce identifiable superlattice peaks for a given material system and TEM

sample thickness seems largely unestablished. Even if SRO is not the source of the observed intensities, its presence may be closely linked to the nucleation and (lack of) growth of stacking faults and twins [1, 12] and indirectly reflected in these observations. TEM characterization may also reveal the presence of SRO through other indirect signatures such as the transition from wavy to planar slip [4].

## ACKNOWLEDGMENTS

This work was supported by the US Department of Energy, Office of Science, Office of Basic Energy Sci-

ences, Materials Sciences and Engineering Division under contract No. DE-AC02-05CH11231 as part of the Damage-Tolerance in Structural Materials (KC13) program. Work at the Molecular Foundry was supported by the US Department of Energy, Office of Science, Office of Basic Energy Sciences under the same contract.

- 
- [1] Ding, J., Yu, Q., Asta, M. & Ritchie, R. O. Tunable stacking fault energies by tailoring local chemical order in CrCoNi medium-entropy alloys. *Proc. Natl. Acad. Sci.* **115**, 8919–8924 (2018).
- [2] Schönfeld, B. *et al.* Local order in Cr-Fe-Co-Ni: Experiment and electronic structure calculations. *Phys. Rev. B* **99**, 014206 (2019).
- [3] Kostiuhenko, T., Ruban, A. V., Neugebauer, J., Shapeev, A. & Körmann, F. Short-range order in face-centered cubic VCoNi alloys. *Phys. Rev. Mater.* **4**, 113802 (2020).
- [4] Zhang, R. *et al.* Short-range order and its impact on the CrCoNi medium-entropy alloy. *Nature* **581**, 283–287 (2020).
- [5] Yin, B., Yoshida, S., Tsuji, N. & Curtin, W. A. Yield strength and misfit volumes of NiCoCr and implications for short-range-order. *Nat. Commun.* **11**, 2507 (2020).
- [6] Pei, Z., Li, R., Gao, M. C. & Stocks, G. M. Statistics of the NiCoCr medium-entropy alloy: Novel aspects of an old puzzle. *npj Comput. Mater.* **6**, 1–6 (2020).
- [7] Inoue, K., Yoshida, S. & Tsuji, N. Direct observation of local chemical ordering in a few nanometer range in CoCrNi medium-entropy alloy by atom probe tomography and its impact on mechanical properties. *Phys. Rev. Mater.* **5**, 085007 (2021).
- [8] Walsh, F., Asta, M. & Ritchie, R. O. Magnetically driven short-range order can explain anomalous measurements in CrCoNi. *Proc. Natl. Acad. Sci.* **118**, e2020540118 (2021).
- [9] Chen, X. *et al.* Direct observation of chemical short-range order in a medium-entropy alloy. *Nature* **592**, 712–716 (2021).
- [10] Chen, X., Yuan, F., Zhou, H. & Wu, X. Structure motif of chemical short-range order in a medium-entropy alloy. *Mater. Res. Lett.* **10**, 149–155 (2022).
- [11] Zhou, L. *et al.* Atomic-scale evidence of chemical short-range order in CrCoNi medium-entropy alloy. *Acta Mater.* **224**, 117490 (2022).
- [12] Yu, P., Du, J.-P., Shinzato, S., Meng, F.-S. & Ogata, S. Theory of history-dependent multi-layer generalized stacking fault energy—A modeling of the micro-substructure evolution kinetics in chemically ordered medium-entropy alloys. *Acta Mater.* **224**, 117504 (2022).
- [13] Du, J.-P. *et al.* Chemical domain structure and its formation kinetics in CrCoNi medium-entropy alloy. *Acta Mater.* **240**, 118314 (2022).
- [14] Zhang, M. *et al.* Determination of peak ordering in the CrCoNi medium-entropy alloy via nanoindentation. *Acta Mater.* 118380 (2022).
- [15] Niu, C., LaRosa, C. R., Miao, J., Mills, M. J. & Ghazisaeidi, M. Magnetically-driven phase transformation strengthening in high entropy alloys. *Nat. Commun.* **9**, 1363 (2018).
- [16] Dong, Z., Schönecker, S., Li, W., Chen, D. & Vitos, L. Thermal spin fluctuations in CoCrFeMnNi high entropy alloy. *Sci. Rep.* **8**, 12211 (2018).
- [17] Kim, Y. S., Maeng, W. Y. & Kim, S. S. Effect of short-range ordering on stress corrosion cracking susceptibility of Alloy 600 studied by electron and neutron diffraction. *Acta Mater.* **83**, 507–515 (2015).
- [18] Seol, J. B. *et al.* Short-range order strengthening in boron-doped high-entropy alloys for cryogenic applications. *Acta Mater.* **194**, 366–377 (2020).
- [19] Liu, D. *et al.* Chemical short-range order in Fe<sub>50</sub>Mn<sub>30</sub>Co<sub>10</sub>Cr<sub>10</sub> high-entropy alloy. *Mater. Today Nano* **16**, 100139 (2021).
- [20] Kayani, S. H., Park, S., Kim, J. G., Seol, J. B. & Sung, H. Direct observation of chemical short-range order in 25 wt% Mn steel via transmission electron microscopy. *Scripta Mater.* **213**, 114642 (2022).
- [21] Zhou, D. *et al.* Effects of annealing on hardness, yield strength and dislocation structure in single crystals of the equiatomic Cr-Mn-Fe-Co-Ni high entropy alloy. *Scripta Mater.* **191**, 173–178 (2021).
- [22] Kawamura, M. *et al.* Plastic deformation of single crystals of the equiatomic Cr-Mn-Fe-Co-Ni high-entropy alloy in tension and compression from 10 K to 1273 K. *Acta Mater.* **203**, 116454 (2021).
- [23] Khachaturyan, A. G. *Theory of Structural Transformations in Solids* (Dover, 2008).
- [24] Rangel DaCosta, L. *et al.* Prismatic 2.0 – Simulation software for scanning and high resolution transmission electron microscopy (STEM and HRTEM). *Micron* **151**, 103141 (2021).
- [25] Xiao, H. Z. & Daykin, A. C. Extra diffractions caused by stacking faults in cubic crystals. *Ultramicroscopy* **53**, 325–331 (1994).
- [26] Schönfeld, B., Reinhard, L., Kistorz, G. & Bührer, W.

- Short-Range Order and Atomic Displacements in Ni-20 at% Cr Single Crystals. *Phys. Status Solidi B* **148**, 457–471 (1988).
- [27] Caudron, R. *et al.* *In Situ* diffuse scattering of neutrons in alloys and application to phase diagram determination. *J. phys., I* **2**, 1145–1171 (1992).
- [28] Schönfeld, B. *et al.* X-ray study of diffuse scattering in Ni-20 at% Cr. *Phys. Status Solidi B* **183**, 79–95 (1994).
- [29] Bolloc'h, D. L., Finel, A. & Caudron, R. Concentration dependence of the short-range order in the Ni-V and Pt-V systems. *Phys. Rev. B* **62**, 12082–12088 (2000).
- [30] Staunton, J. B., Johnson, D. D. & Pinski, F. J. Compositional short-range ordering in metallic alloys: Band-filling, charge-transfer, and size effects from a first-principles all-electron Landau-type theory. *Phys. Rev. B* **50**, 1450–1472 (1994).